Conference Proceedings Paper

Quasicrystal Model as Framework for an Order to Disorder Transitions in 2D Systems

Nadezhda L. Cherkas [1] and Sergey L. Cherkas [2,*]

[1] Military Academy of the Republic of Belarus; n_cherkas@mail.ru

[2] Institute for Nuclear Problems, Belarus State University; cherkas@inp.bsu.by

* Correspondence: cherkas@inp.bsu.by; Tel.: +375-17-226-47-39

Abstract: An order to disorder transitions are important for 2D objects such as oxide films with cellular porous structure, honeycomb, graphene, Bénard cells in liquid and artificial systems consisting of colloid particles on a plane. For instance, solid films of the porous alumina represent almost regular quasicrystal structure. We show that in this case the radial distribution function is well described by the quasicrystal model, i.e. the smeared hexagonal lattice of the two dimensional ideal crystal with inserting some amount of defects into the lattice. Another example is a system of the hard disks in a plane which illustrates the order to disorder transitions. It is shown, that the coincidence with the distribution function, obtained by the solution of the Percus-Yevick equation is achieved by the smoothing of the square lattice and injecting the defects of the vacancy type into it. However, better approximation is reached when the lattice is a result of a mixture of the smoothened square and hexagonal lattices. Impurity of the hexagonal lattice is considerable at the short distances. Dependences of the lattices constants, smoothing widths and impurity on the filling parameter are found. Transition to the order looks as an increasing of the hexagonal lattice contribution and decreasing of smearing.

Keywords: order to disorder transitions; 2D objects; radial distribution function; quasicrystal model; wavelet; porous aluminium oxide; hard disks in a plane

1. Introduction

It is well known that for particles on a plane interacting via a certain potential the existence of crystal, i.e., a system with periodicity, is impossible at nonzero temperature [1–4]. However there exist number of 2D objects in nature which exhibit crystalline like ordering. Usually these objects have non perfect crystalline structure and a question arises about transition from order to disorder. It is noteworthy that the order–disorder transition was experimentally studied from the general point of view in [5], where the destruction of a graphene layer by the electron beam was analyzed. A continuous transition from the crystalline state to the glassy state occurred as a result of irradiation. At the initial stage of irradiation, individual defects appear in the lattice. Then, the glassy (disordered) regions surrounding crystallites (perfectly oriented regions) emerge. In the disordered regions, the destruction of the order initially manifested itself of pentagonal and tetragonal cells instead of the hexagonal ones. The area occupied by crystallites decreases with an increase in the irradiation dose.

As it was believed in [5], experiment confirms the validity both of the two competing theories of the order–disorder transition. They involve, on the one hand, the theory of crystallites [6] (according to which a amorphous substance incorporates crystal-like agglomerates linked by disordered regions) and, on the other hand, the theory of random networks (see review [7]), which assumes that the order is destroyed throughout the entire volume of a substance, so that the crystal lattice

transforms into random chains of atoms due to the distortion and break of some bonds. Thus, it follows from the experiment [5] that single defects are formed at the initial stages. Then the theory of crystallites proves to be valid; further, the theory of random networks starts to work. In this study we propose to take into consideration two mechanisms in order to simulate the radial distribution function of 2D systems. The first implies the formation of vacancy-type defects (i.e., the absence of atoms in some lattice sites), when the crystal lattice structure is retained. The second mechanism corresponds to the destruction of the crystal lattice and is implemented via peak broadening in the structure factor and limitation of the peak height at large wave numbers. The method of crystal lattice smearing proposed in [8] was used to construct an empirical radial distribution function. This method was applied to describe the structure of some simple liquids [9–15]. A similar method of smearing of coordination circles was used to describe artificial 2D crystals [16,17]. Here we consider a slightly different method consisting in the random shifting of the crystal nodes.

2. Radial Distribution Function for Porous Aluminum Oxide Layer

Oxide films with cellular porous structure are formed upon the electrochemical oxidation (anodiza- tion) of aluminum and many aluminum alloys in solutions of various acids. The film thickness may be as large as several hundreds of micrometers, while the pore radius size is several tens of nanometers. Such films have been studied for more than 50 years. They are widely applied as anticorrosion, wear-resistant, electro-insulating, and decorative coatings in microelectronic and optical devices, membranes, and sensors. Under a combination of certain conditions, including acid concentration and type, a film can be grown as an ordered array of cylindrical pores similar to a 2D periodic lattice [18–20]. Various theories describing the ordered structure of pores in aluminum oxide fabricated by anodization have been proposed [21,22]. However, presently there is no complete understanding of the regularities of ordered structure formation; hence, the radial distri-bution function of pores cannot be calculated theoretically. At the same time, the knowledge of the radial distribution function is necessary for optical calculations. For example, the effective refractive index of a medium consisting of porous aluminum oxide depends strongly on the radial distribution function [23]. The imaginary part of the effective refractive index is particularly sensitive to the form of the radial distribution function. As for the experimental determination of the radial distribution function using an electron microscope, its accuracy is limited by the finite sizes of a sample [24]. Thus, one needs semi-empirical models to describe the radial distribution function of pores in porous aluminum oxide. It is reasonable to suggest that the ordered structure of porous aluminum oxide is something intermediate between the 2D crystal and amorphous substance. Therefore, it is meaningful to study porous aluminum oxide from the viewpoint of general principles of the order–disorder transition [25,26].
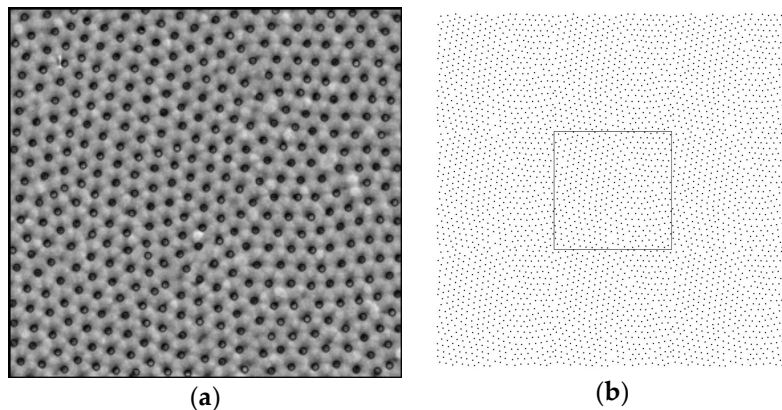

(a)　　　　　　　　　　　　　　(b)

Figure 1. (**a**) Photograph of the sample of porous aluminumoxide layer from Ref. [8]. Circles around pore centers are plotted; (**b**) Array of pore centers obtained by a parallel translation of the pore

centers in the initial array along the coordinate axes and the diagonals of the sample. The region containing pore centers in the starting sample is selected by a rectangle.

Let us first analyze a real sample of porous aluminum oxide in order to understand the form of the radial distribution function that should be sought after. In practice, there is generally a photograph of the sample, which can be analyzed by statistical methods [24]. In this study, we used the electron microscopy image obtained in [27] and shown in Figure 1 (a). There are computer programs for determining the centers of cylindrical holes [24], which analyze the contrast of pixels. However, we plotted the pore centers manually. The average distance between pores in the sample was on the order of 100 nm [27]. To avoid edge effects and, at the same time, to have an opportunity to calculate the radial correlation function at somewhat larger distances, we increased the sample area by parallel translations along the coordinate axes and diagonals (Figure 2). Although this increase in the area gave rise to a certain error, it allowed increasing the distance at which the correlation function can be calculated. Then, using a computer program, we counted the number of pores between the circles of radii ρ and $\rho + d\rho$ (including the pores of the extended sample) in the neighborhood of each selected pore of the initial sample. Such calculation was performed for each pore of the initial sample, and then the average value was found. A binary distribution function of the pore density distribution was calculated by the formula

$$g(\rho) = \frac{\Delta N}{\pi \left((\rho + \Delta\rho)^2 - \rho^2 \right)} \frac{N}{N+1}, \tag{1}$$

here ΔN is the number of pores in the region between the circles of radii ρ and $\rho + d\rho$, whereas N is the number of pores in the sample. The correction factor $N/(N+1)$ in (1) takes into account the fact that the selected pore cannot be situated within its environment. Radial distribution function $W(\rho)$ related to the function $g(\rho)$ by the expression $W(\rho) = g(\rho)/n_0$ is usually used, where n_0 is the average surface density of pores in the sample. Thus, the calculation of the radial distribution function is similar to the calculation in the Monte Carlo method, except for the fact that the sample in the Monte Carlo method is generated while the method at hand deals with an experimental sample. As a result, the radial distribution function was obtained. However, the statistical uncertainty and the error due to edge effects restrict the direct use of this function for optical calculations, since they give rise to errors in the calculation of integrals. At the same time, this accuracy is quite sufficient to construct an empirical distribution function by comparison with the experimental one. A further objective of our study was to derive a smooth empirical distribution function, which could be used in optical calculations. A starting point of our approach is the binary distribution function of particles for an ideal 2D crystal with a certain hexagonal lattice shown in Fig. 2(a). The crystal structure is described, e.g., in [16,25,26]. The two-particle distribution function g(r) is a sum of the Dirac delta-function terms:

$$\tilde{g}(\boldsymbol{\rho}) = \sum_i \delta^{(2)}(\boldsymbol{\rho} - \boldsymbol{\rho}_i), \tag{2}$$

where $\delta^{(2)}(\boldsymbol{\rho})$ represents a two-dimensional delta-function by Dirac, $\boldsymbol{\rho}_i$ is position vectors of particles in an ideal lattice. The particles are situated in the nods of the crystalline lattice. Summation in the formula (2) is performed over all the particles, except one, being in an origin of coordinates. As we have one particle on a cell an average density of the particles in an ideal crystal is easily calculated: $\tilde{n}_0 = \dfrac{1}{S} = \left(\dfrac{ma^2}{4} \tan \dfrac{\pi}{m} \right)^{-1}$, where S is an area of a crystal cell, a is a lattice constant, i.e. diameter of a circle inscribed into the cell, as it is shown in Figure 2, m is the number of edges of a cell.
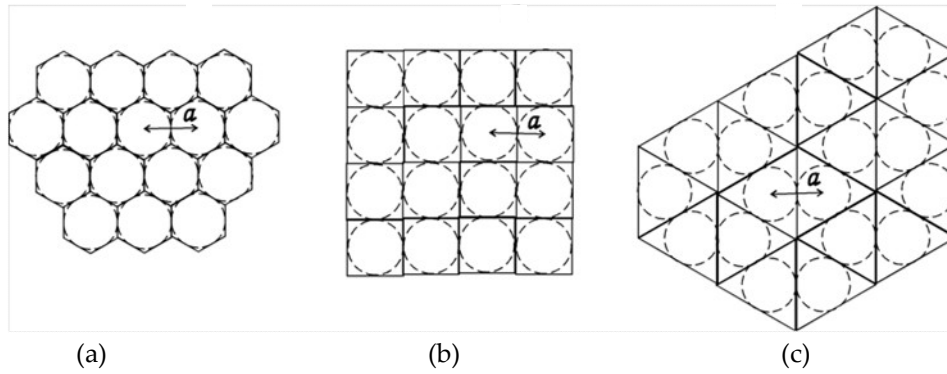
Figure 2. The two-dimensional lattices: hexagonal (a), square (b), triangular (c).

Correlation function is denoted as $\tilde{K}(\boldsymbol{\rho}) = \tilde{g}(\boldsymbol{\rho}) - \tilde{n}_0$. To proceed from an order (an ideal crystal) to disorder, we suggests formation of the defects of the vacancy type at the first stage. This means that there exists a probability of lacking of a particle in a node. As a result, the distribution function takes the form

$$\tilde{\tilde{g}}(\boldsymbol{\rho}) = \begin{cases} n_0 + \tilde{\tilde{K}}(\boldsymbol{\rho}) = n_0 + \left(\sum_i \delta^{(2)}(\boldsymbol{\rho} - \boldsymbol{\rho}_i) - \tilde{n}_0 \right) e^{-\lambda(\rho - D_{\min})}, & \rho > D_{\min}, \\ 0 & , \quad \rho < D_{\min}, \end{cases} \tag{3}$$

where $\tilde{\tilde{g}}(\boldsymbol{\rho})$ denotes a distribution function at this first stage, n_0 is the surface density of the particles in a sample and $D_{\min}$ is a distance at which it is known that the distribution function is apparently zeros. The formula (3) suggests that the correlation function $\tilde{K}(\boldsymbol{\rho})$ of an ideal crystal is exponentially restricted at large ρ. Besides, it is taken into account, that $\tilde{\tilde{g}}(\boldsymbol{\rho})$ should have the correct asymptotic at infinity, where it is equal to n_0, and should be equal to zero at $\rho < D_{\min}$. At the second stage the spreading of a lattice by means of some integral transformation is carried out

$$g(\boldsymbol{\rho}) = \int\limits_{\rho' > D_{\min}} G(\boldsymbol{\rho}, \boldsymbol{\rho}') \tilde{\tilde{g}}(\boldsymbol{\rho}') d^2 \boldsymbol{\rho}', \quad \rho > D_{\min}, \tag{4}$$

where we have supposed

$$G(\boldsymbol{\rho}, \boldsymbol{\rho}') = \Delta(\rho) \exp\left(-\frac{(\boldsymbol{\rho}' - \boldsymbol{\rho})^2}{2\sigma^2(\rho)} \right). \tag{5}$$

The integral transformation given by Eqns. (4), (5) maps a set of the integrable functions defined on the two-dimensional region $\rho > D_{\min}$ into itself. At $\rho < D_{\min}$ $g(\boldsymbol{\rho}) = 0$ as in (3). Normalising factor $\Delta(\rho)$ is equal to

$$\Delta(\rho) = \left(\int\limits_{\rho' > D_{\min}} \exp\left(-\frac{(\boldsymbol{\rho}' - \boldsymbol{\rho})^2}{2\sigma^2(\rho)} \right) d^2 \boldsymbol{\rho}' \right)^{-1} = \left(2\pi \int\limits_{D_{\min}}^{\infty} \exp\left(-\frac{(\rho'^2 + \rho^2)}{2\sigma^2(\rho)} \right) I_0\left(\frac{\rho'\rho}{\sigma^2(\rho)} \right) \rho' d\rho' \right)^{-1},$$

where $I_0(z)$ is a zero order modified Bessel function of the first kind. The above expression for $\Delta(\rho)$ implies that the action of the transformation (4) action to the function equal to some constant do not change it. As a result one comes to

$$g(\boldsymbol{\rho}) = n_0 + \Delta(\rho) \left(\sum_i \exp\left(-\lambda(\rho_i - D_{\min}) - \frac{(\boldsymbol{\rho}_i - \boldsymbol{\rho})^2}{2\sigma^2(\rho)} \right) - \right.$$
$$\left. -2\pi\tilde{n}_0 \int_{D_{\min}}^{\infty} \exp\left(-\lambda(\rho' - D_{\min}) - \frac{(\rho'^2 + \rho^2)}{2\sigma^2(\rho)} \right) I_0\left(\frac{\rho'\rho}{\sigma^2(\rho)} \right) \rho' d\rho' \right). \tag{6}$$

We do not consider an orientation order and a loss of it here and, an averaged $\bar{g}(\rho) = \dfrac{1}{2\pi} \displaystyle\int_0^{2\pi} g(\boldsymbol{\rho})d\varphi$ over orientation of the vector $\boldsymbol{\rho}$ (polar coordinates is used) is considered. Thus, all the directions are equivalent, and the pare distribution function depends only on distance ρ. The radial distribution function $W(\rho) = \bar{g}(\rho)/n_0$ is usually considered. As a result we come to the following formula

$$W(\rho) = 1 + 2\pi\Delta(\rho) \left(\frac{1}{n_0} \sum_i N_i \exp\left(-\lambda(\rho_i - D_{\min}) - \frac{(\rho_i^2 + \rho^2)}{2\sigma^2(\rho)} \right) I_0\left(\frac{\rho_i\rho}{\sigma^2(\rho)} \right) - \right.$$
$$\left. -\frac{\tilde{n}_0}{n_0} \int_{D_{\min}}^{\infty} \exp\left(-\lambda(\rho' - D_{\min}) - \frac{(\rho'^2 + \rho^2)}{2\sigma^2(\rho)} \right) I_0\left(\frac{\rho'\rho}{\sigma^2(\rho)} \right) \rho' \iota \tag{7}$$

where summation is performed not over the nods, but over coordination circles on which the nodes are situated and, N_i is the number of the nods laying on each i-th coordination circle.
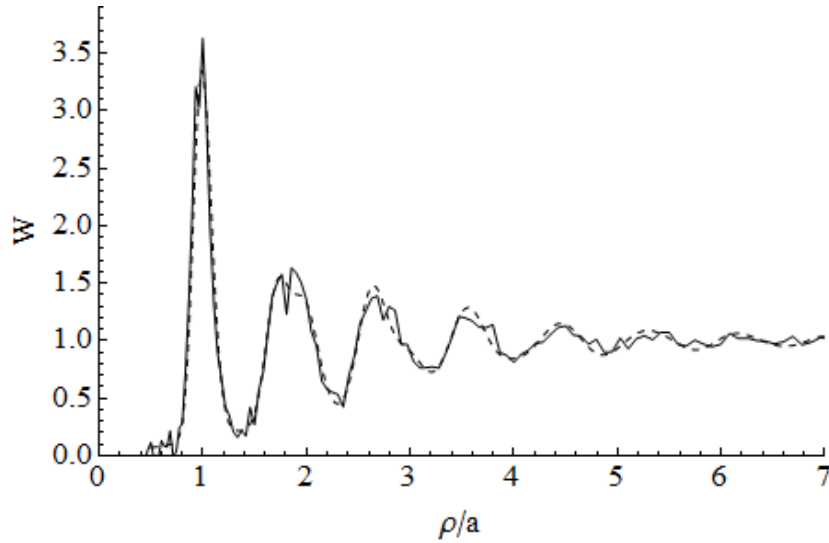

Figure 3. Radial distribution function of pores in porous aluminum oxide: experimental sample [8] (solid curve) and our calculation (dashed curve).

The result of calculation is shown in Figure 3. The following parameters were used $\sigma(\rho) = 0.0877(a\rho)^{1/2}$, $n_0 = 0.965\tilde{n}_0$, $D_{\min} = 0.4a$, $\lambda = 0.2/a$. One can see that there is a good agreement with the experimental radial distribution function obtained by counting the number of pores in the sample shown in Fig. 1(a).

3. Hard Disks in a Plane

Let us consider a quiet different system, namely, hard disk fluid. This system, on the one hand, attracts mathematicians and physicists with its simplicity, while, on the other hand, it is a test bed to explore transition from the order to the disorder, hard disc liquid to hexatic, the liquid to hexagonal

crystal and the liquid-to-maximally random jammed state [28-32]. The pair distribution function characterizes the important features of the system as compressibility and the equation of state [33,34]. The limiting case of a distribution function of hard disks under increasing of disk concentration is the hexagonal lattice, i.e. a two-dimensional crystal. It is reasonable, that at densities, close to maximum, the two-particle distribution function can be described in a frame of quasicrystal model by the smearing of a hexagonal lattice. At lower concentrations of particles the methods of integral equations [35], based on a decoupling of the Bogolubov chain of the equations, work well. In particular, the Percus-Yevick integral equation [29,35] is usually used. There question arises whether quasicrystal model works not only in the proximity to a crystal, but also at the medium concentrations? Below we consider the quasicrystal model at the range of medium concentration of disks.

3.1. Comparison with the Solutions of the Percus-Yevick Equation

Disk concentration is characterized by the packing fraction $\eta = n_0 \pi R^2$, where R is a disk radius. It is evident that the value of $D_{\min} = 2R$, because the centers of the two hard disks are separated at least by this distance. Value of the lattice constant a has to depend on η. The question arises which lattice should be smeared to obtain the correct pair distribution function? It turns out to be that the qualitative agreement with the solutions of the Percus-Yevick equation is reached if a square lattice is smeared. From the other hand it is obvious, that under increasing of the disk density we should come to a hexagonal lattice. To take this into account, we suggest the following model:

$$W(\rho) = W_{squ}(\rho)(1 - e^{-b\rho^2}) + W_{gex}(\rho)e^{-b\rho^2} , \qquad (8)$$

i.e. radial distribution function is superposition of the two terms obtained by the spreading of the square and hexagonal lattices with the weight functions depending on distance. The functions $W_{squ}(\rho)$ and $W_{gex}(\rho)$ are calculated by Equation (7). Parameter $\sigma(\rho)$ determining spreading of the lattice depends on distance as $\sigma(\rho) = \gamma\sqrt{\rho}$ that is the nodes situated further are smeared stronger. Results of the comparison with the solutions of the Percus-Yevick equation are shown in Figures. 4,5. It is should be noted, that the Percus-Yevick equation is not solved analytically for hard disks on planes thus, numerical methods therefore were used. It seems very interesting that the "tails" of the distribution function shown in Figures 4(b), 5(b) are modeled with high accuracy. Percus-Yevick equation stops to work at filling parameter about 0.6, which restricts present consideration. However, it is evident that the parameterization of the radial distribution function given by Equation (7) will be useful for higher disk concentrations, where phase transitions occur. Table 1 contains all the parameters used in the calculations. For simplicity we consider that the parameters γ and λ determining smearing and an amount of defects-vacancies are same for both lattices, however constants of the lattices are taken different. As one could see spreading and number of defects decreases with the increasing of η, i.e. system tends from a disorder to an order.

Table 1. Constants of lattices a_{squ} and a_{gex} for modeling quasicrystal an allocation radial distribution function at various block coefficients η, and also other parameters figuring in formulas (6), (7).

η	$a_{squ}/(2R)$	$a_{gex}/(2R)$	$\gamma/(2R)^{1/2}$	$2\lambda R$	$b(2R)^2$
0.62	1.04	1.1	0.158	0.027	0.4
0.6	1.056	1.12	0.176	0.03	0.41
0.55	1.095	1.14	0.192	0.1	0.45
0.5	1.11	1.2	0.2	0.2	0.53
0.45	1.112	1.3	0.209	0.5	0.7
0.4	1.115	1.6	0.213	0.9	1.1
0.35	1.117	2.1	0.224	1.4	0.75
0.3	1.12	2.3	0.236	2	0.6[1]

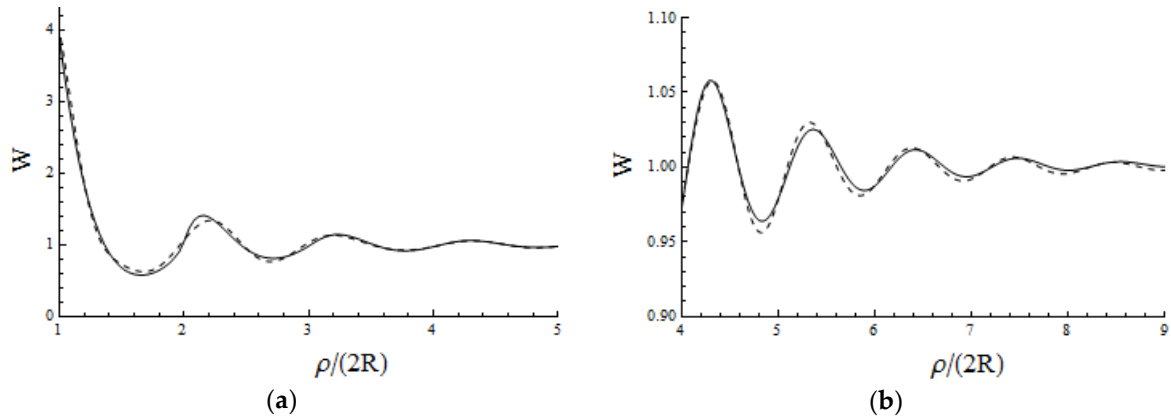[1] All the quantities are dimensionless.

Figure 4. Radial distributions function for filling $\eta = 0.62$, in a range $\rho \in \{1,5\}$ (a), in a range $\rho \in \{4,9\}$ ("a tail of the distribution function") (b). Solid line is a solution of the Percus-Yevick equation, dashed line is the quasicrystal model.
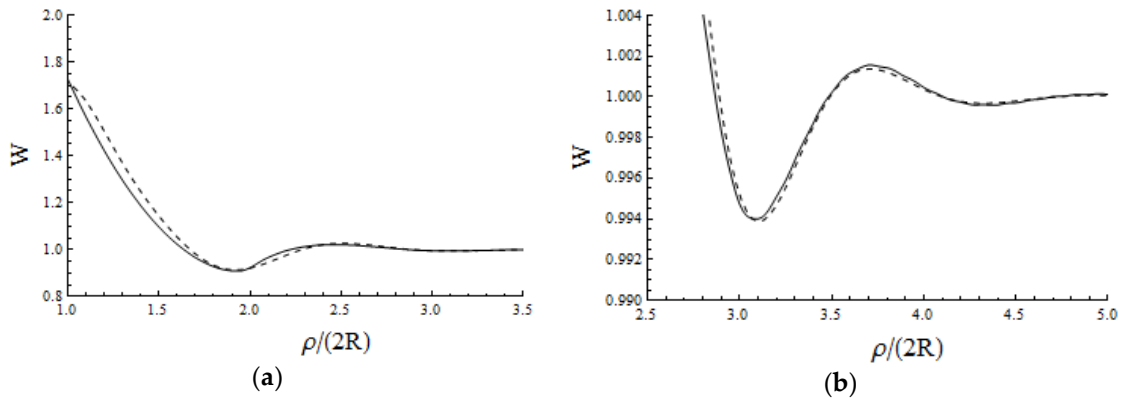

Figure 5. Radial distribution functions for filling $\eta = 0.3$, in a range $\rho \in \{1,3.5\}$ (a), in a range $\rho \in \{2.5,5.0\}$ ("a tail of the distribution function") (b). Solid line is a solution of the Percus-Yevick equation, dashed line is the quasicrystal model. **.**

4. Conclusions

Radial distribution function parameterization, based on the quasicrystall model is presented. This parameterization describes on the same footing as porous aluminum oxide, so as 2-D hard disk fluid. The quasicrystall model is based on the two effects: the first one is the vacancy type defects formation and the second one is the destroying of the crystal lattice by the smearing. The successes of this paramerization shows that even liquid of the hard disks contain features of a crystal. The model will serve as a tool for the description of the phase transitions in the 2-D fluids. From the other hand, it could be base for variational methods, because the parameters describing spreading, defects probability and lattice constants could be found by minimization of some functional [36].

Conflicts of Interest: The authors declare no conflict of interest.

References

1. Peierls, R.E. Transformation tempretures. *Helv. Phys. Acta Suppl.* **1934**, *2*, 81–83.
2. Landau, L.D. On the theory of phase transitions I. *Phys. Z. Sowjet.* **1937**, *11*, 26–35.
3. Landau, L.D. On the theory of phase transitions II. *Phys. Z. Sowjet.* **1937**, *11*, 545–555.
4. Mermin, N.D. Crystalline order in two dimensions. *Phys.Rev.* **1968**, *176*, 250–254.

5. Eder, F.R.; Kotakoski, J.; et al. A journey from order to disorder – atom by atom transformation from graphen to 2D carbon glass. *Sci. Rep.* **2014**, *4*, 4060.

6. Warren, B.E. X-ray Diffraction Study of the Structure of Glass. *Chem. Rev.* **1940**, *26*, 237–255.

7. Wright, A.C., Thorpe, M.F. Eighty years of random networks. *Phys. Status Solidi B* **2013**, *250*, 931–936.

8. Prins, G.A., Petersen, H. Theoretical diffraction patterns corresponding to some simple types of molecular arrangement in liquids. *Physica* **1936**, 3, 147–153.

9. Glauberman, A.E. On the theory of a local order in liquids. *Zh. Eksp. Teor. Fiz.* **1952**, *22*, 249–250.

10. Tsvetkov, V.P. About structure of the liquid metals. *Izv. Vyssh. Uchebn. Zaved., Ser. Fiz.* **1960**, *1*, 145–154.

11. Franchetti, S. On a model for monoatomic liquids. *Nuovo Cim. B* **1968**, *55*, 335–347.

12. Medvedev, N.N.; Naberukhin, Yu.I. Description of the radial distribution function of liquid argon in the quasi-crystalline model of liquids. *Phys. Chem. Liquids* **1978**, *8*, 167–187.

13. Baer, S. Form of the radial distribution function and the structure factor, derived from the "structural diffusion" model for liquids. *Physica* A **1978**, *91*, 603–611.

14. Skryshevskii, A.F. *Structural Analysis of Liquids and Amorphous Solids.* Vysshaya Shkola, Moscow, 1980, p. 49.

15. Medvedev, N.N.; Naberukhin, Yu.I.; Semenova, I.Yu. The radial distribution function and structure factor of liquid and amorphous gallium as described by the quasi-crystalline model. *J. Non-Cryst. Solids* **1984**, *64*, 421–432.

16. Miskevich, A.A.; Loiko V.A. Coherent transmission and reflection of a two-dimensional planar photonic crystal. *Zh. Eksp. Teor. Fiz.* **2011**, *140*, 5–20.

17. Cherkas, N.L.; Cherkas, S.L. Model of the radial distribution function of pores in a layer of porous aluminum oxide. *Crystallogr. Rep.* **2016**, *61*, 285–290.

18. Masuda, H.; Fukuda, K. Ordered metal nanohole arrays made by a two-step replication of honeycomb structures of anodic alumina. *Science* **1995** *268*, 1466–1468.

19. Jessensky, O.; Müller, F.; Gösele, U. Self-organized formation of hexagonal pore arrays in anodic alumina. *Appl. Phys. Lett.* **1998**, *72*, 1173–1175.

20. Nielsch, K.; Choi, J.; Schwirn, K. Self-ordering Regimes of Porous Alumina: The 10 Porosity Rule. *Nano Lett.* **2002**, *2*, 677–680.

21. Parkhutik, V.P.; Shershulsky, V.I. Theoretical modelling of porous oxide growth on aluminium. *J. Phys. D* **1992**, *25*, 1258–1263.

22. Singh, G.K.; Golovin, A.A.; Aranson I.S. Formation of self-organized nanoscale porous structures in anodic aluminum oxide. *Phys. Rev. B* **2006**, *73*, 205422.

23. Cherkas, N.L. Electromagnetic wave in a medium consisting of parallel dielectric cylinders. *Opt. Spektrosk.* **1996**, *81*, 990–996.

24. Yakovleva, N.M.; Yakovlev, A.N.; Gafiyatullin, M.M.; *et al*. Computer diagnostics of the mesoscopic structure of the nanoporous oxides of aluminum. *Zavod. Lab. Diagn. Mater.* **2009**, *75*, 21–26.

25. Kaatz, F.H. Measuring the order in ordered porous arrays: can bees outperform humans? *Naturwissenschaften* **2006**, *93*, 374–378.

26. Vodopivec, A.; Kaatz, F.H.; Mohar, B. Topographical distance matrices for porous arrays. *J. Math. Chem.* **2010**, *47*, 1145–1153.

27. Lutich, A.A.; Gaponenko, S.V.; Gaponenko, N.V.; *et al*. Anisotropic light scattering in nanoporous materials: A photon density of states effect. *Nano Lett.* **2004**, *4*, 1755–1758.

28. Fernandez, J.F.; Alonso, J.J.; Stankiewicz, J. Melting of systems of hard disks by Monte Carlo simulations. *Phys. Rev. E.* **1997**, *55*, 750-764.

29. Adda-Bedia, M.; Katzav, E.; Vella, D. Solution of the Percus-Yevick equation for hard disks. *J. Chem. Phys.* **2008**, *128*, 184508.

30. Kapfer, S.C.; Krauth, W. Sampling from a polytope and hard-disk Monte Carlo. *J. Phys.: Conf. Ser.* **2013**, *454*, 012031.

31. Gaal, A.T. Long-range order in a hard disk model. *Electron. Comm. Probab.* **2014**, *19*, 1–9.

32. Atkinson, S.; Stillinger, F.H.; Torquato, S. Existence of isostatic, maximally random jammed monodisperse hard-disk packings. *Proc. National Acad. Sci. U.S. Am.* **2014**, *111*, 18436–18441.

33. Engel, M.; Anderson, J.A.; Glotzer, S.C.; *et al*. Hard-disk equation of state: First-order liquid-hexatic transition in two dimensions with three simulation methods. *Phys. Rev. E* **2013**, *87*, 042134.

34. Sokołowski, S. A note on the two-dimensional radial distribution function. *Czec. J. Phys. B* **1978**, *28*, 713-720.

35. Kovalenko, N.P.; Fisher, I.Z. Method of integral equations in statistical theory of liquids. *Uspekhi Fizicheskih Nauk*, **1972**, *108*, 209–239.

36. Arinshtein, E.A. A model of the liquid-crystal phase transition and the quasicrystal model of liquid. *Theor. Math. Phys.* **2007**, *151*, 571–585.